ESI:

Carboxylate-rich Multidentate Hybrid Ligands in Mn^{II} Complexes for Water Oxidation Reactions

C. R. Raymond Gan,[a] Zhaolin Liu,[b] Shi-Qiang Bai,[b] Kian Soo Ong,[b] and T. S. Andy Hor,*[bc]

[a]*NUS Graduate School for Integrative Sciences and Engineering (NGS), Center for Life Sciences (CeLS), #05-01, 28 Medical Drive Singapore 117456, Singapore* [b]*Institute of Materials Research and Engineering, Agency for Science, Technology and Research, 3 Research Link, S117602. Singapore.* [c]*Department of Chemistry, National University of Singapore, 3 Science Drive 3, S117543.*

[*]*Email: andyhor@nus.edu.sg*

1. ESI-MS studies of complexes 1 to 4

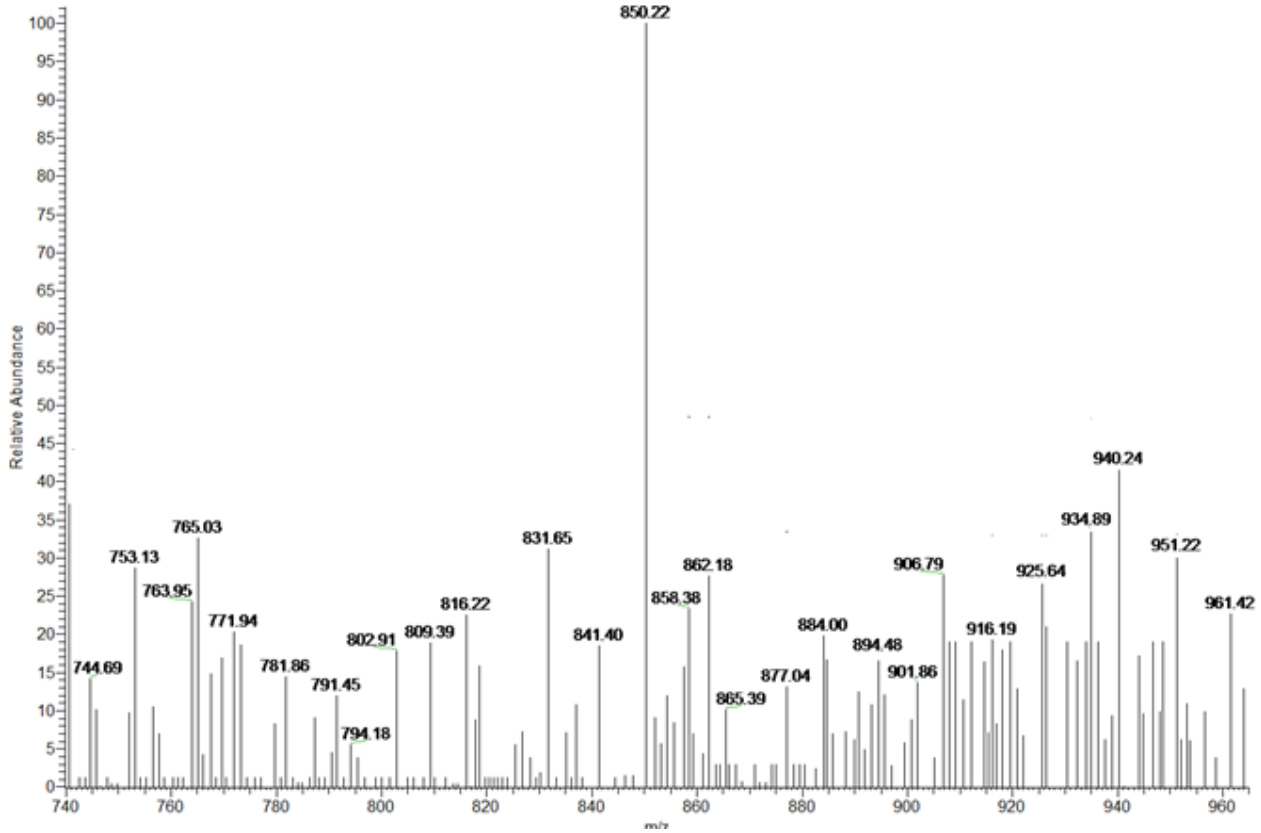

Fig. S1 ESI-MS spectrum of complex **1**.

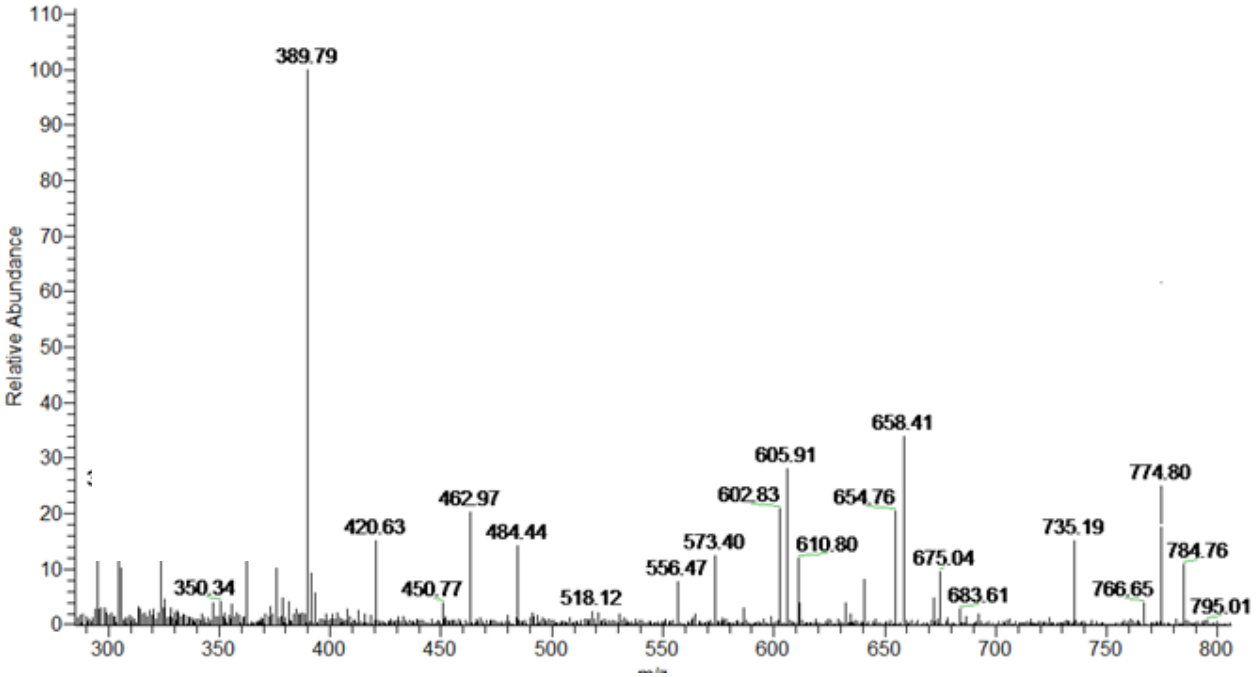

Fig. S2 ESI-MS spectrum of complex **2**.

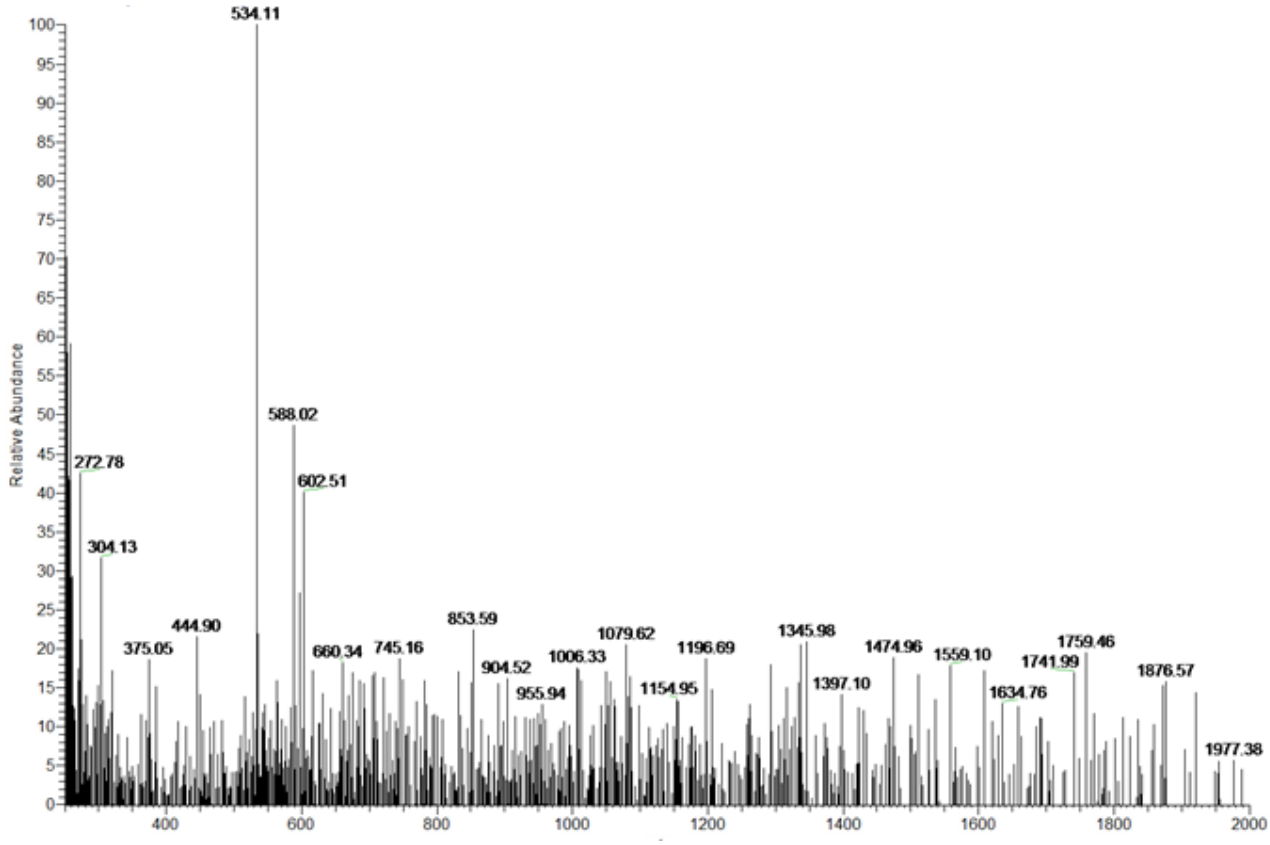

Fig. S3 ESI-MS spectrum of complex **3**.

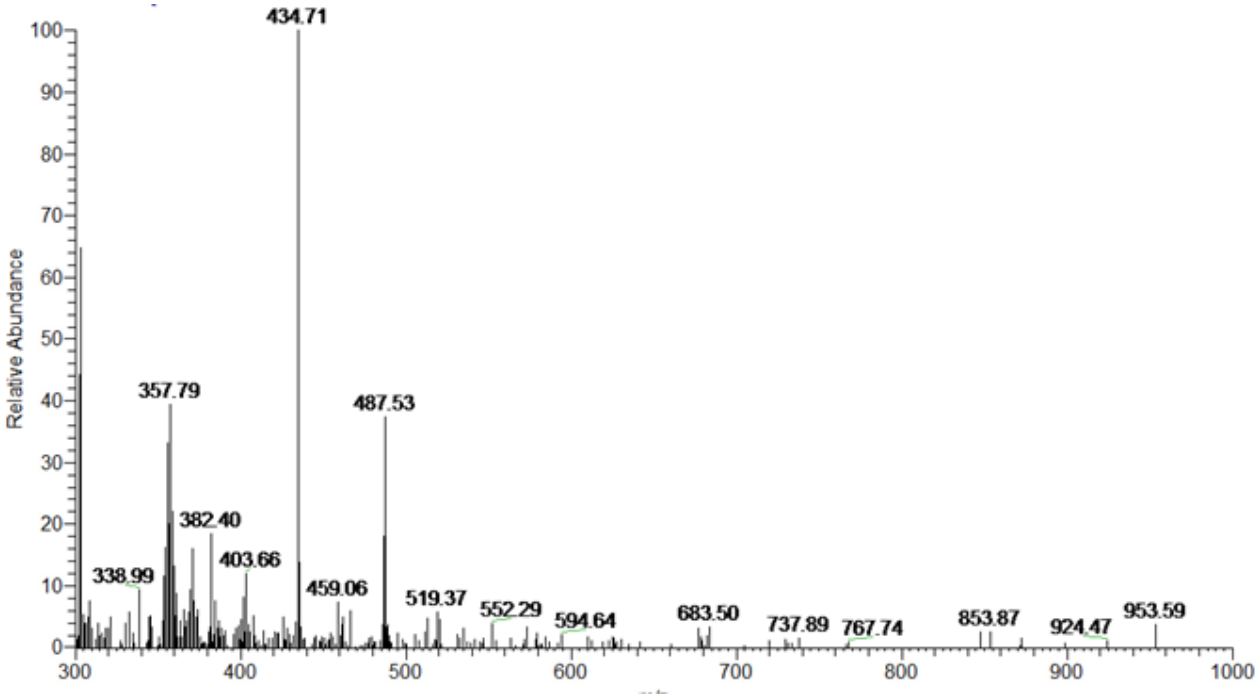

Fig. S4 ESI-MS spectrum of complex **4**.

2. Clark cell

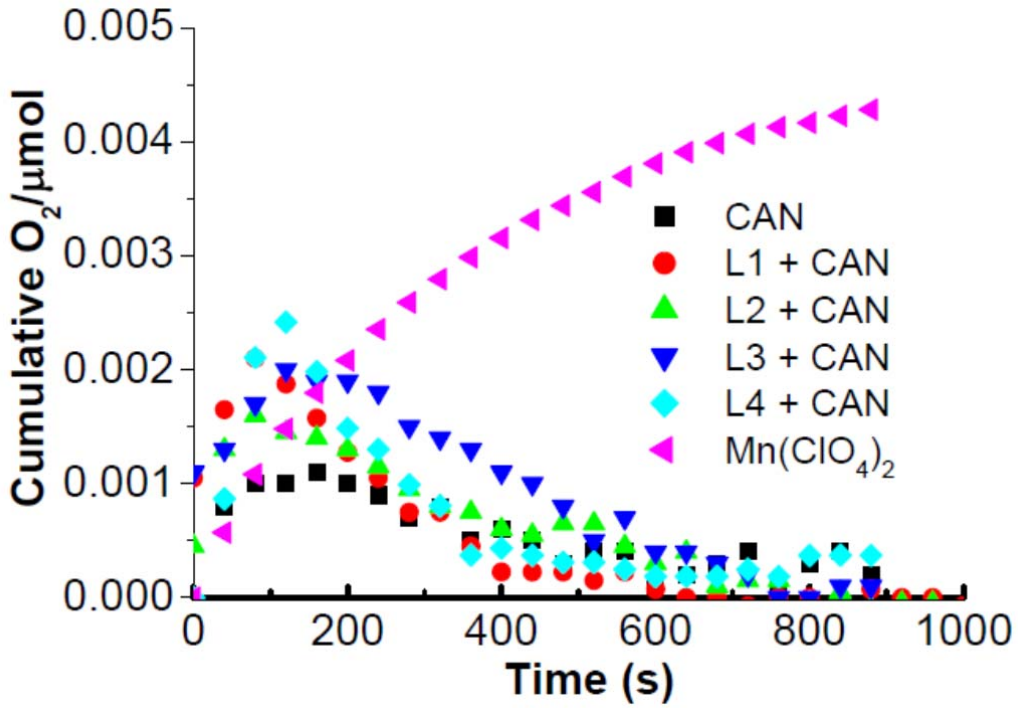

Fig. S5 O_2 evolution of controls.

3. Gas chromatography

3.1 Reaction in $^{16}OH_2$

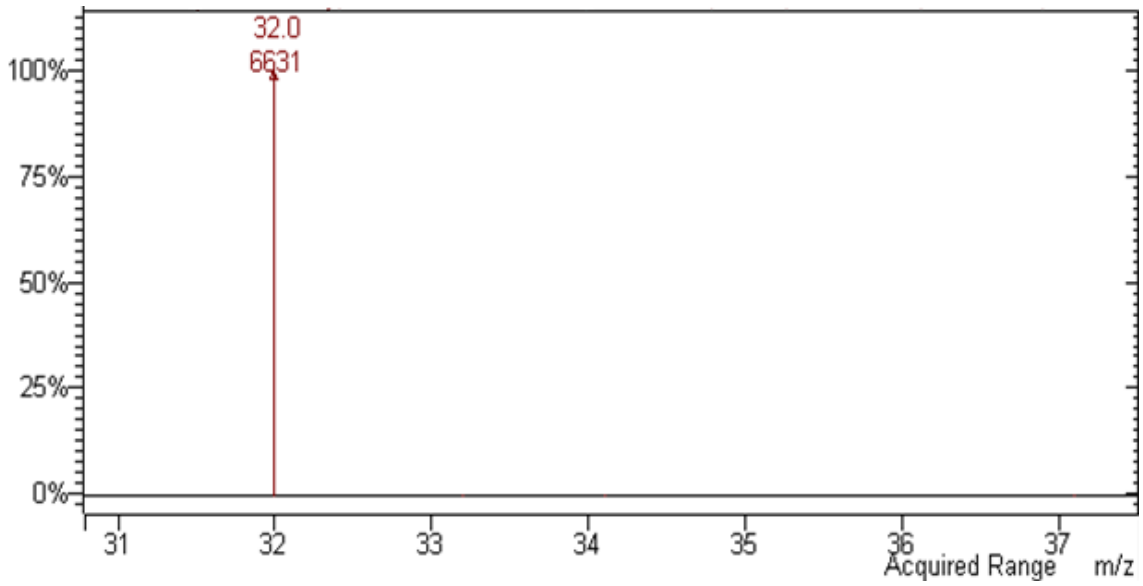

Fig. S6 GCMS spectrum of background atmospheric air in argon purged vial as control.

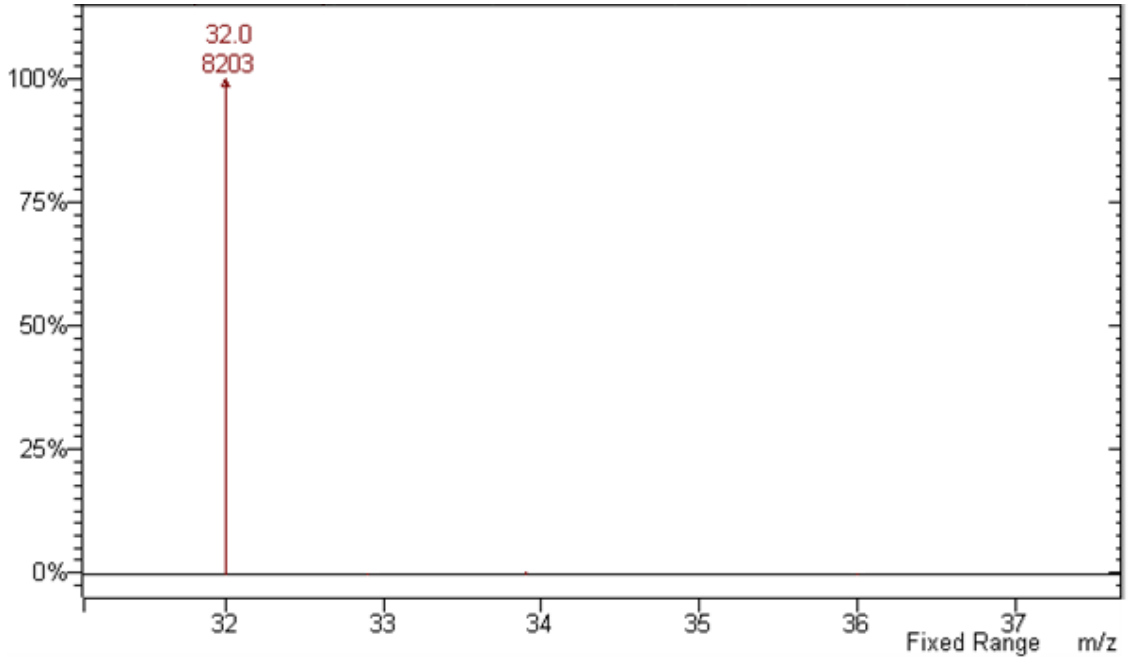

Fig. S7 GCMS spectrum of the headspace upon reacting complex **1** with 80 excess of CAN.

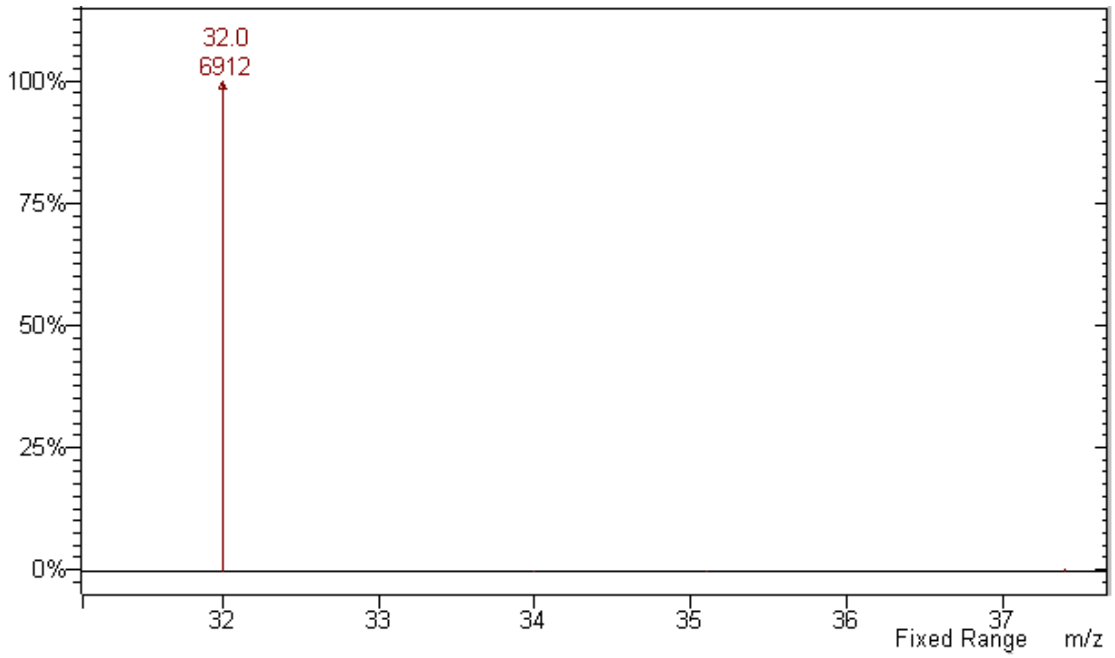

Fig. S8 GCMS spectrum of the headspace upon reacting complex **2** with 80 excess of CAN.

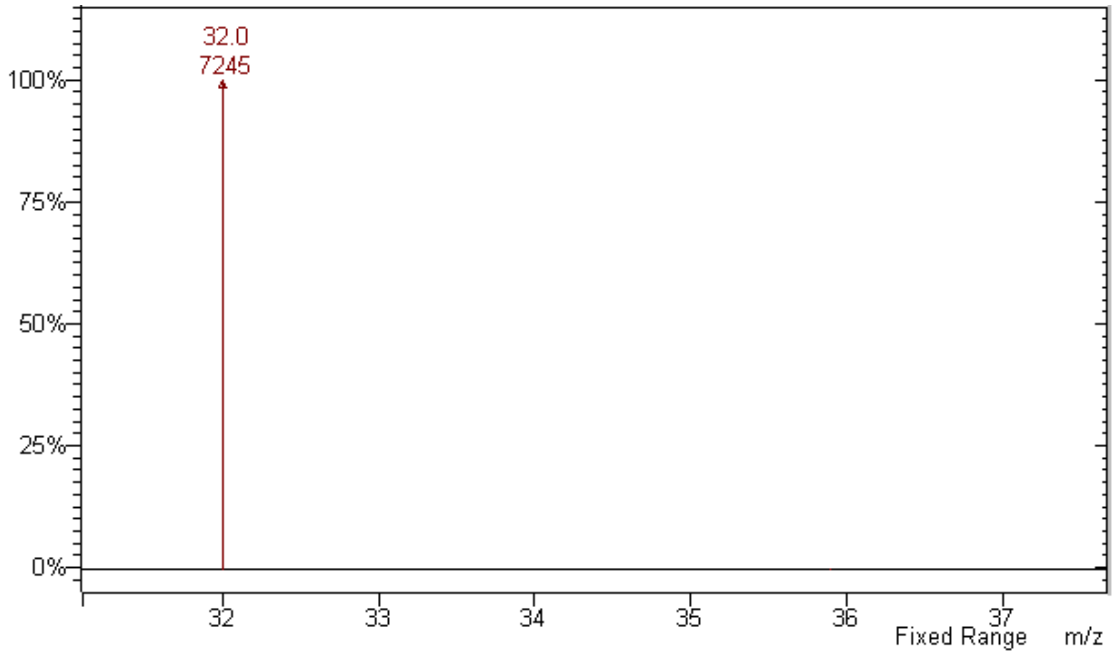

Fig. S9 GCMS spectrum of the headspace upon reacting complex **3** with 80 excess of CAN.

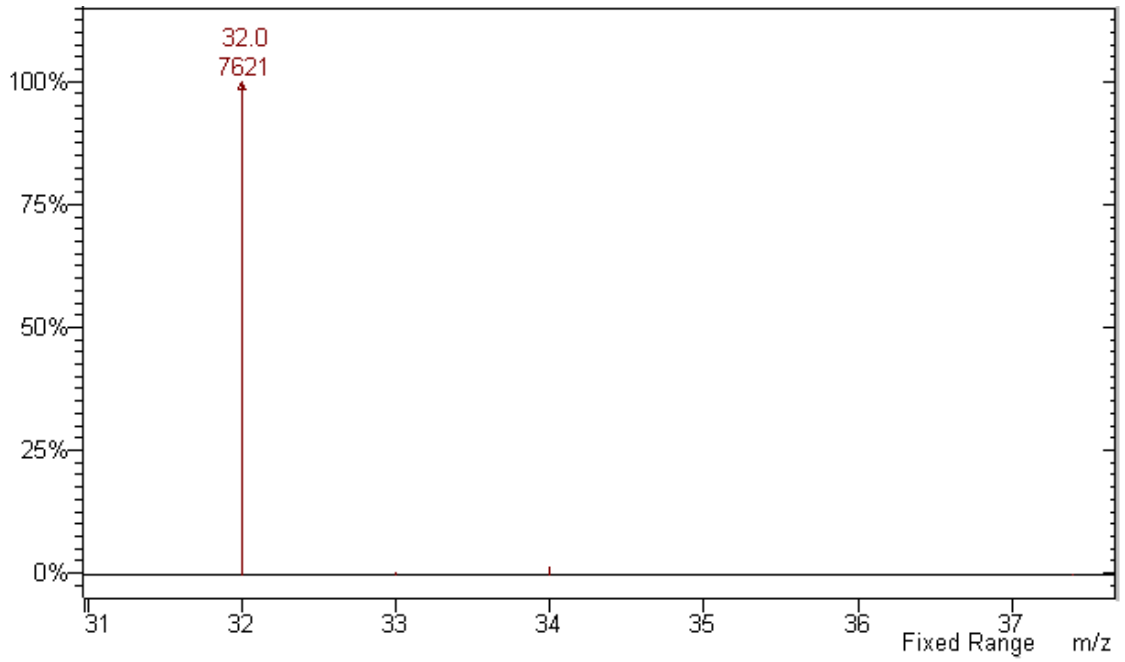

Fig. S10 GCMS spectrum of the headspace upon reacting complex **4** with 80 excess of Ce^{4+}.

3.2 Reaction in $^{18}OH_2$ (95%)

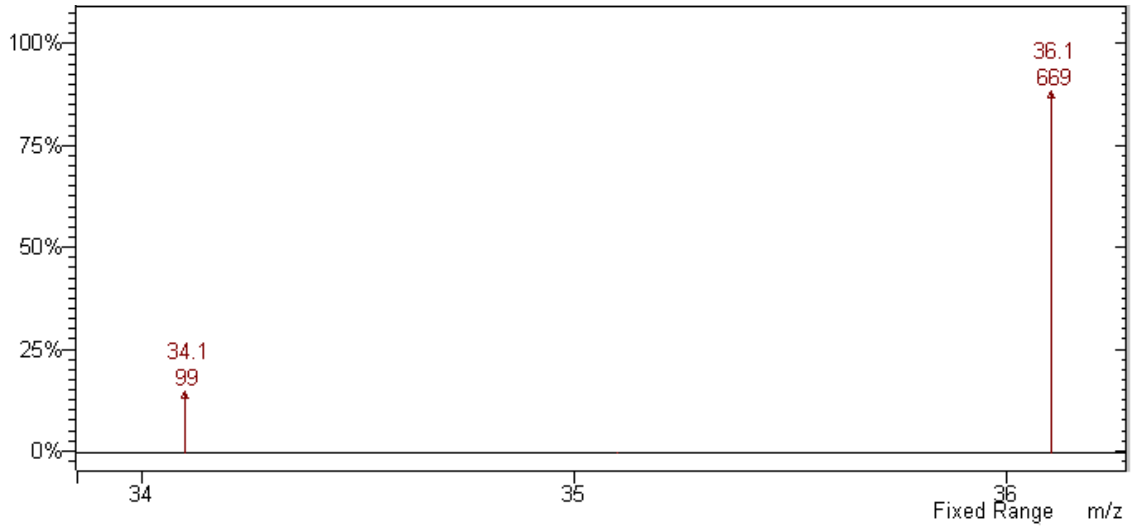

Fig. S11 GCMS spectrum of the headspace upon reacting complex **1** with 80 eq. of CAN.

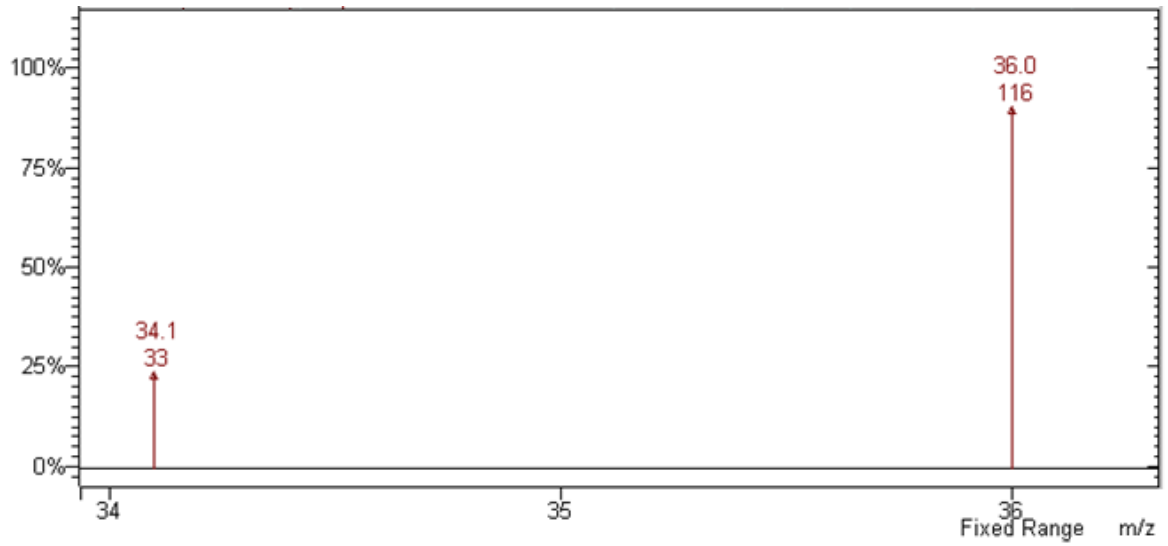

Fig. S12 GCMS spectrum of the headspace upon reacting complex **2** with 80 eq. of CAN.

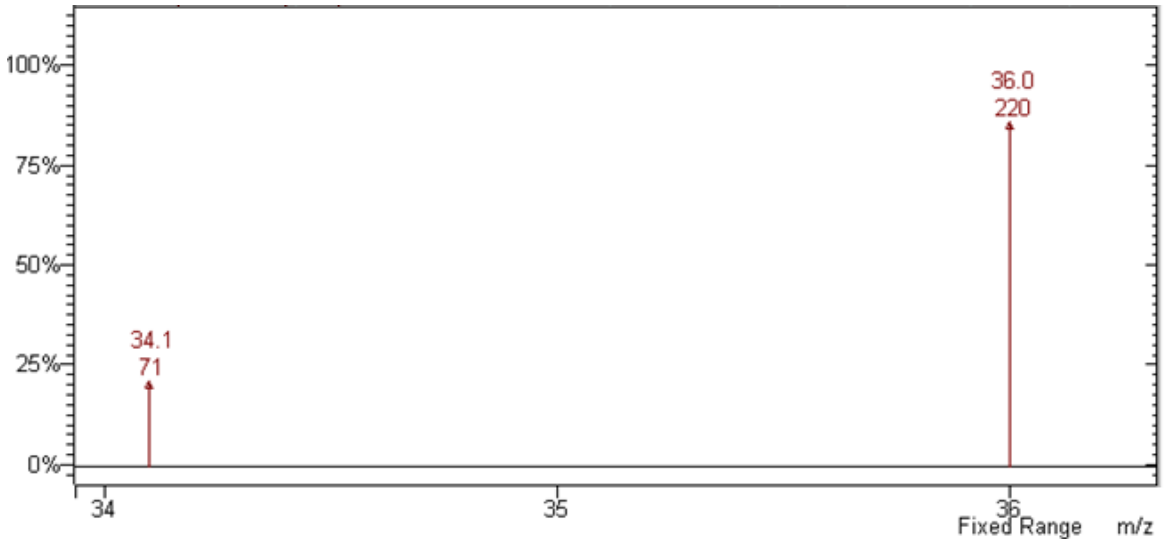

Fig. S13 GCMS spectrum of the headspace upon reacting complex **3** with 80 eq. of CAN.

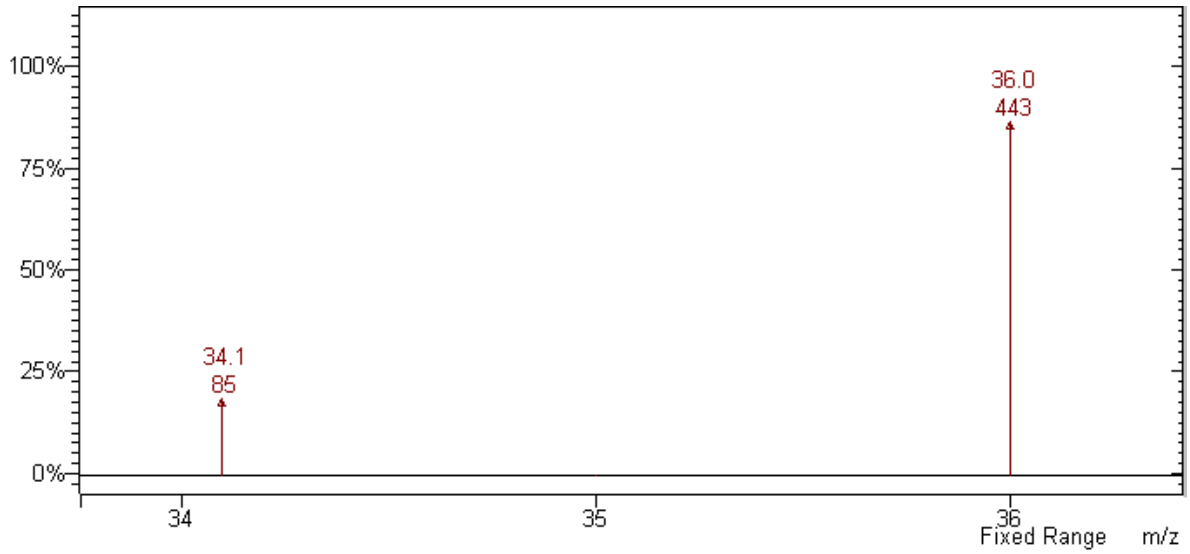

Fig. S14 GCMS spectrum of the headspace upon reacting complex **4** with 80 eq. of CAN.

4. EDS composition

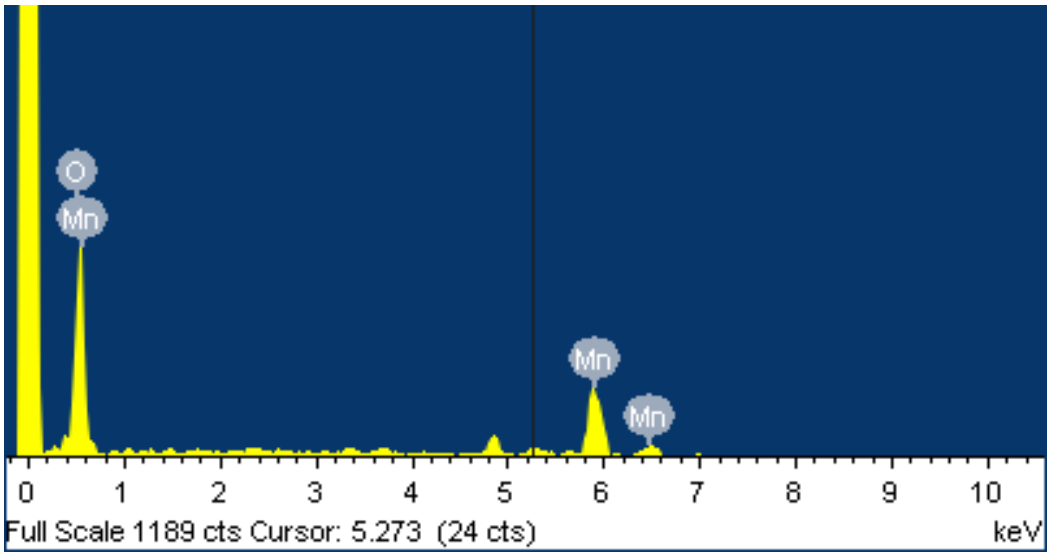

Fig. S15 EDS composition of MnO_2 formed in-situ from reaction of **1** and 80 eq. CAN.

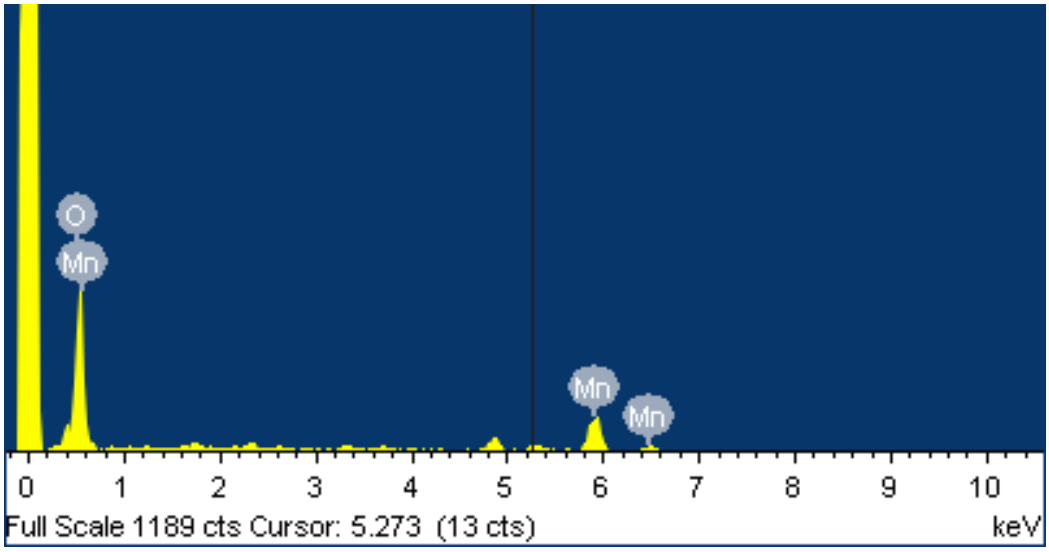

Fig. S16 EDS composition of MnO_2 formed in-situ from reaction of **2** and 80 eq. CAN.

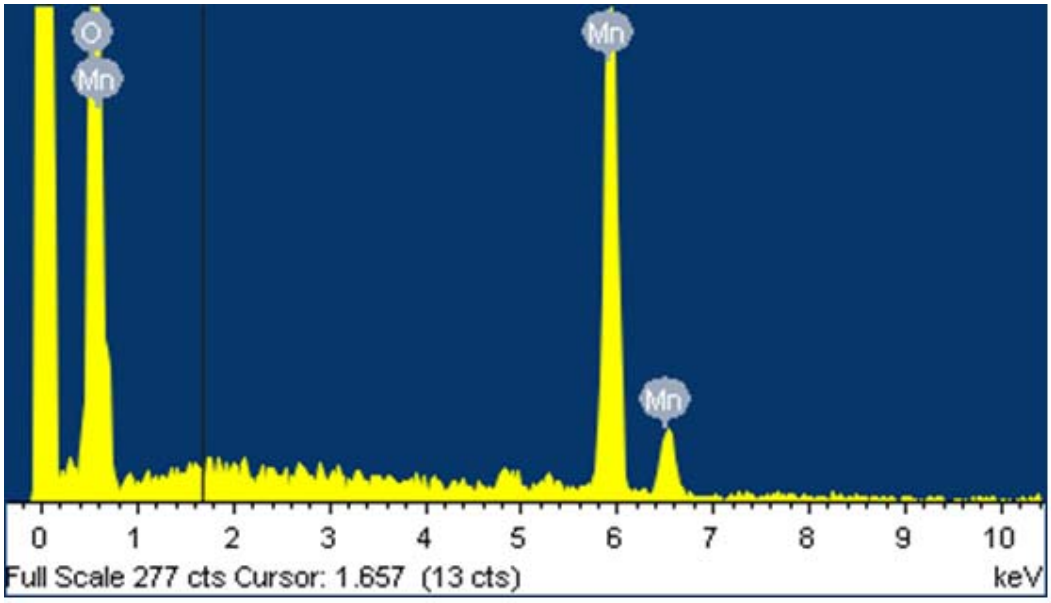

Fig. S17 EDS composition of MnO_2 formed in-situ from reaction of **3** and 80 eq.CAN.

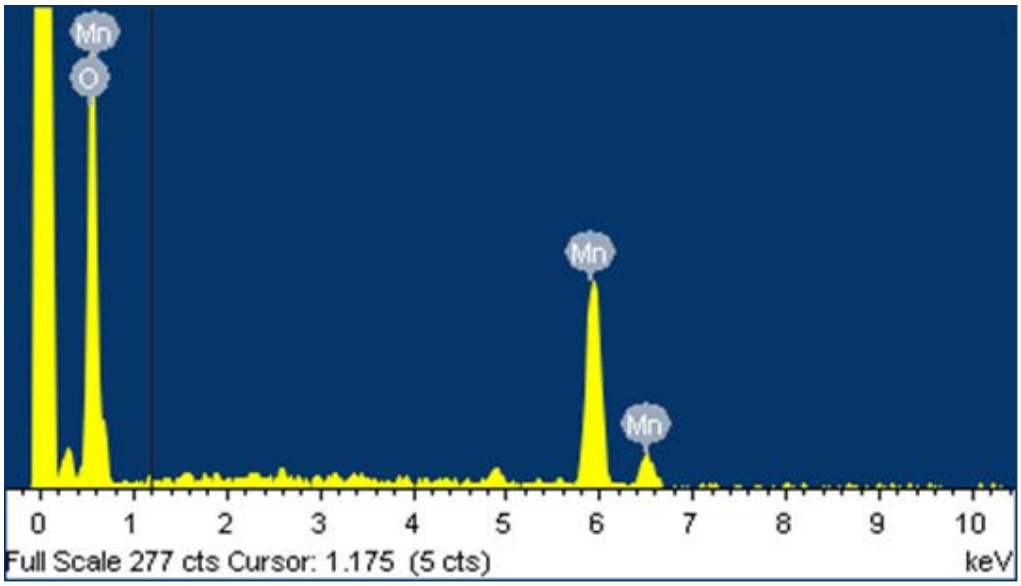

Fig. S18 EDS composition of MnO_2 formed in-situ from reaction of **4** and 80 eq. CAN.

5. ESI-MS studies of the reaction between complexes 1 to 4 with 2 eq. of CAN.

The concentration of the complexes was 0.59mM while the concentration of the CAN solution added was 1.1mM to make up 2.5 ml of reactive solution that rapidly turns brown due to oxidation of Mn^{II}, the solution upon mixing should be immediately injected into the mass spectrometer.

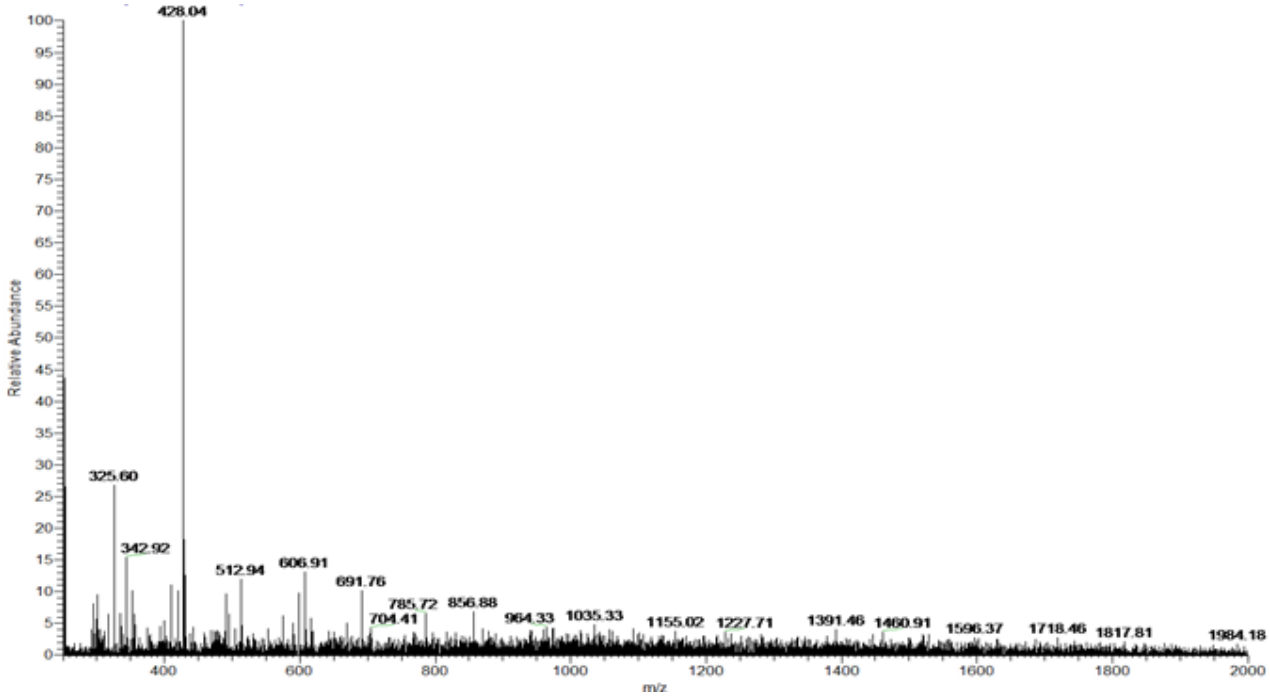

Fig. S19 ESI-MS spectrum of complex **1** after adding two equivalent of CAN.

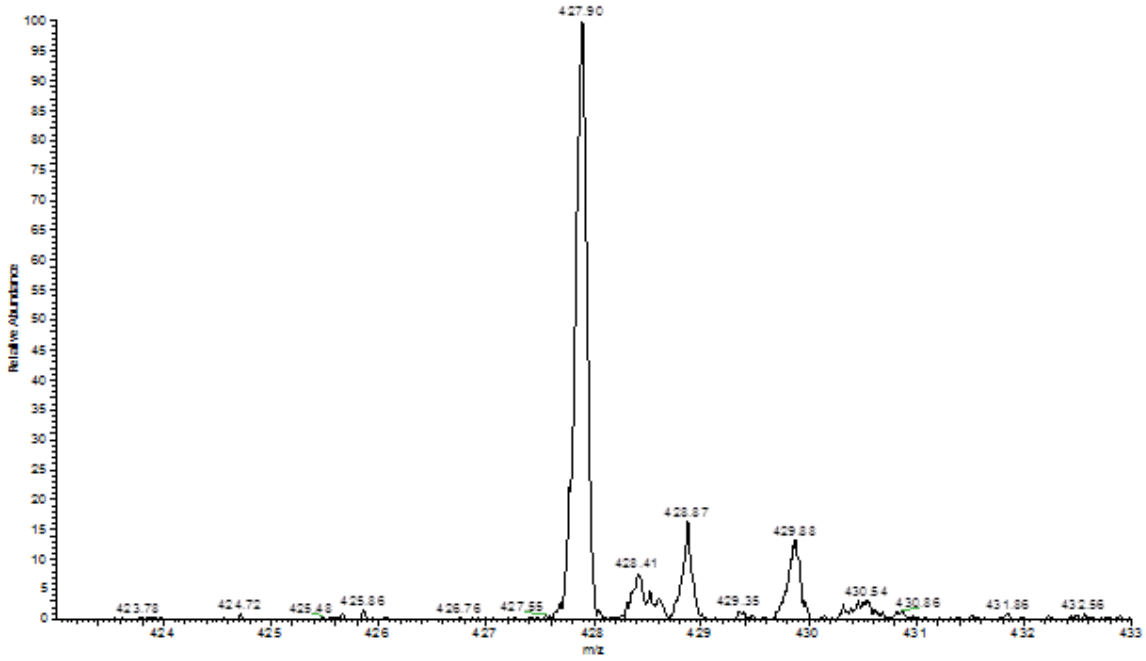

Fig. S20 Isotopic pattern of the dominant intermediate species in the ESI-MS spectrum of complex **1** after adding two equivalent of Ce^{IV}.

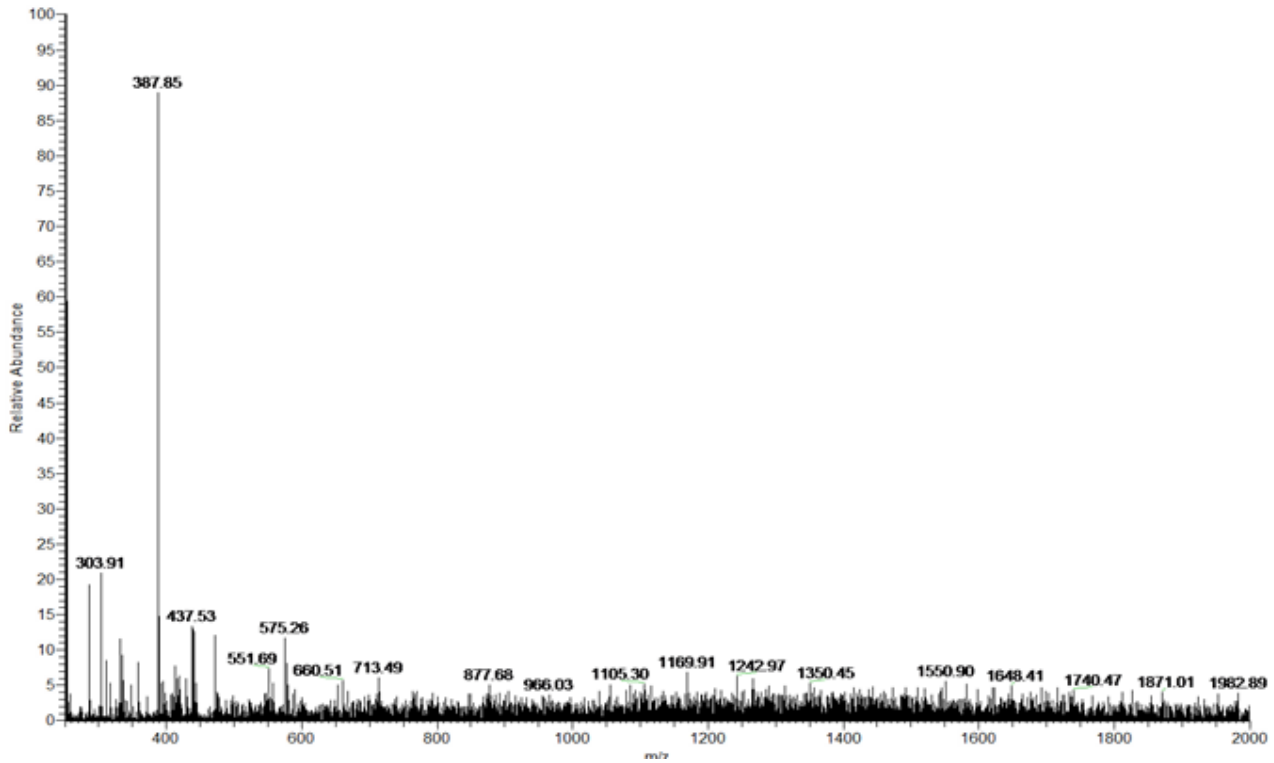

Fig. S21 ESI-MS spectrum of complex **2** after adding two equivalent of CAN.

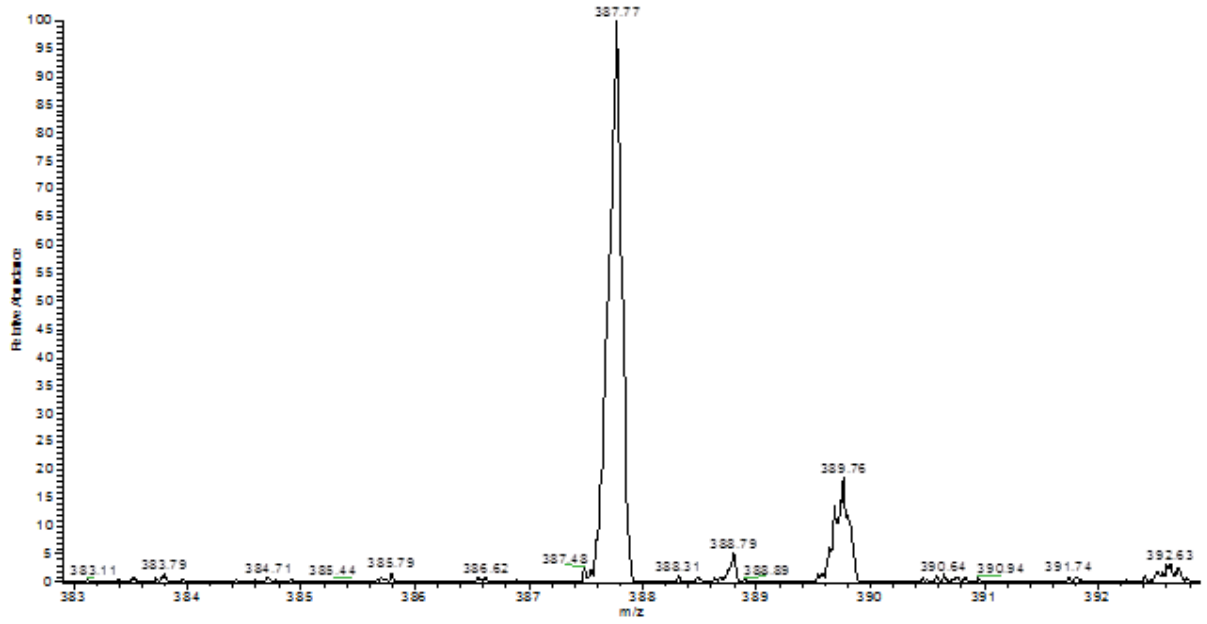

Fig. S22 Isotopic pattern of the dominant intermediate species in the ESI-MS spectrum of complex **2** after adding two equivalent of Ce^{IV}.

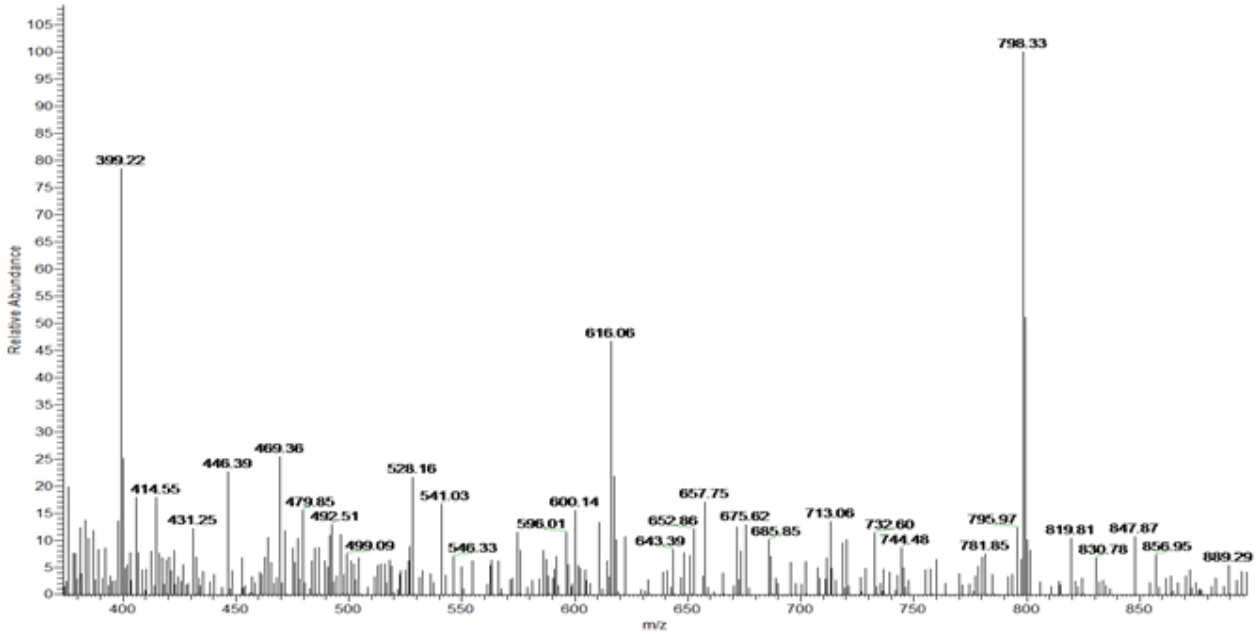

Fig. S23 ESI-MS spectrum of complex **3** after adding two equivalent of CAN.

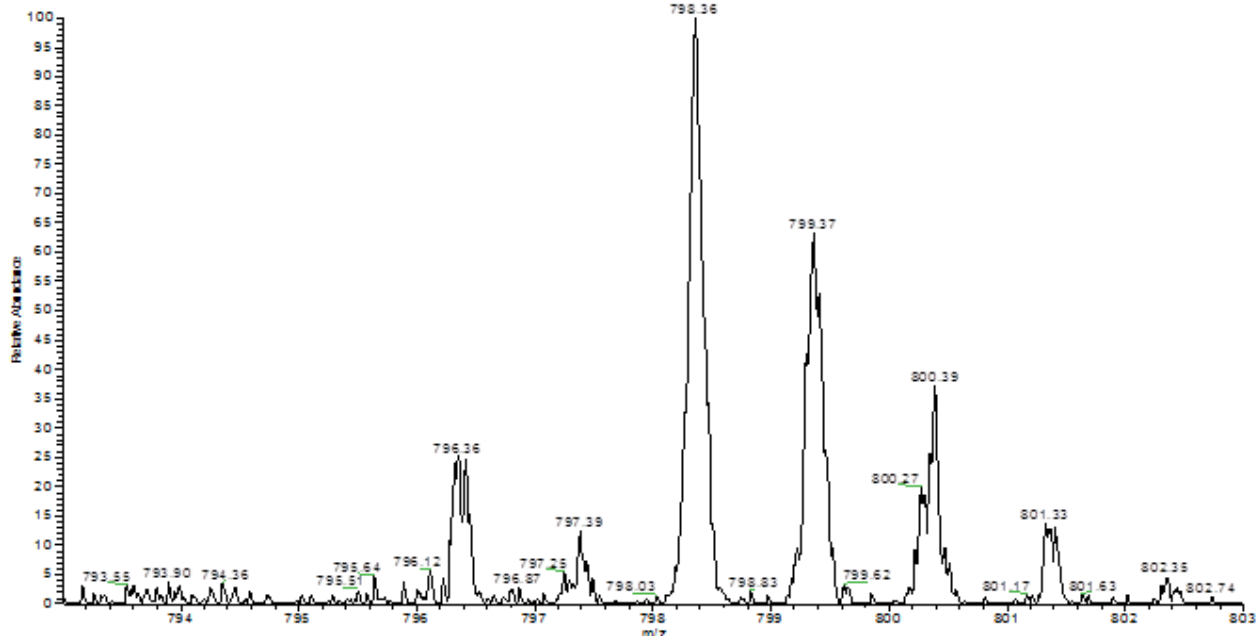

Fig. S24 Isotopic pattern of the dominant intermediate species of 798.36 m/z in the ESI-MS spectrum of complex **3** after adding two equivalent of Ce^{IV}.

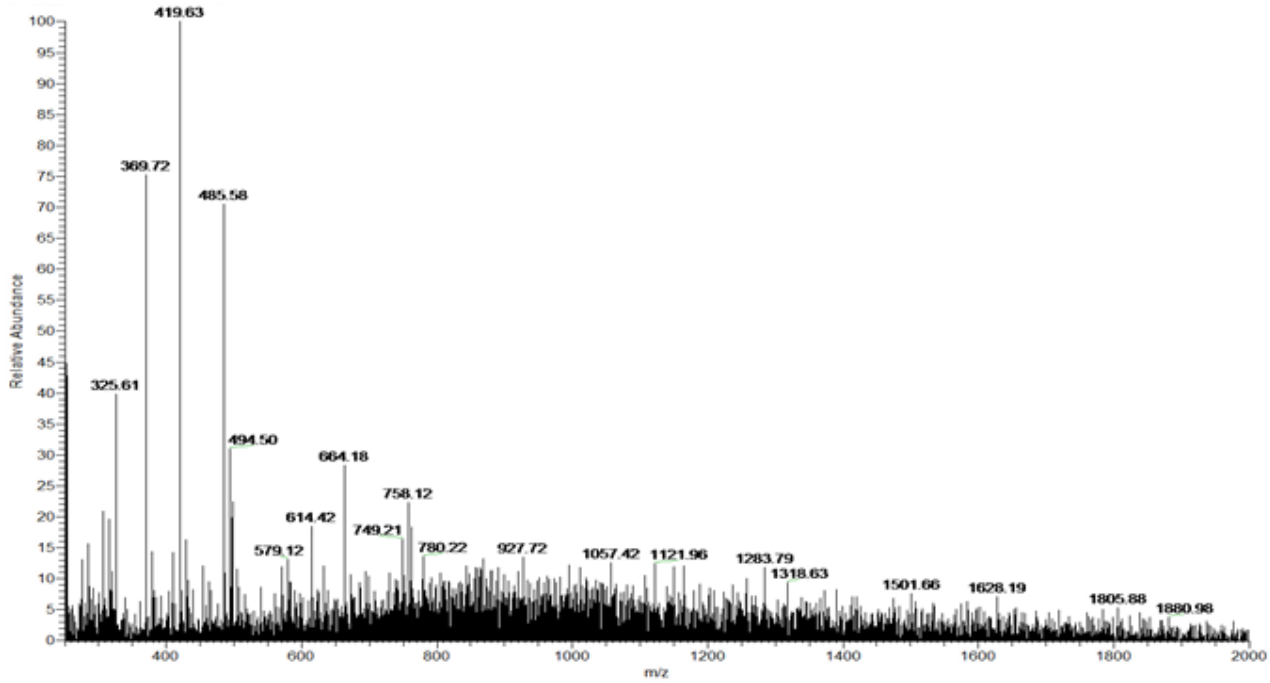

Fig. S25: ESI-MS spectrum of complex **4** after adding two equivalent of CAN.

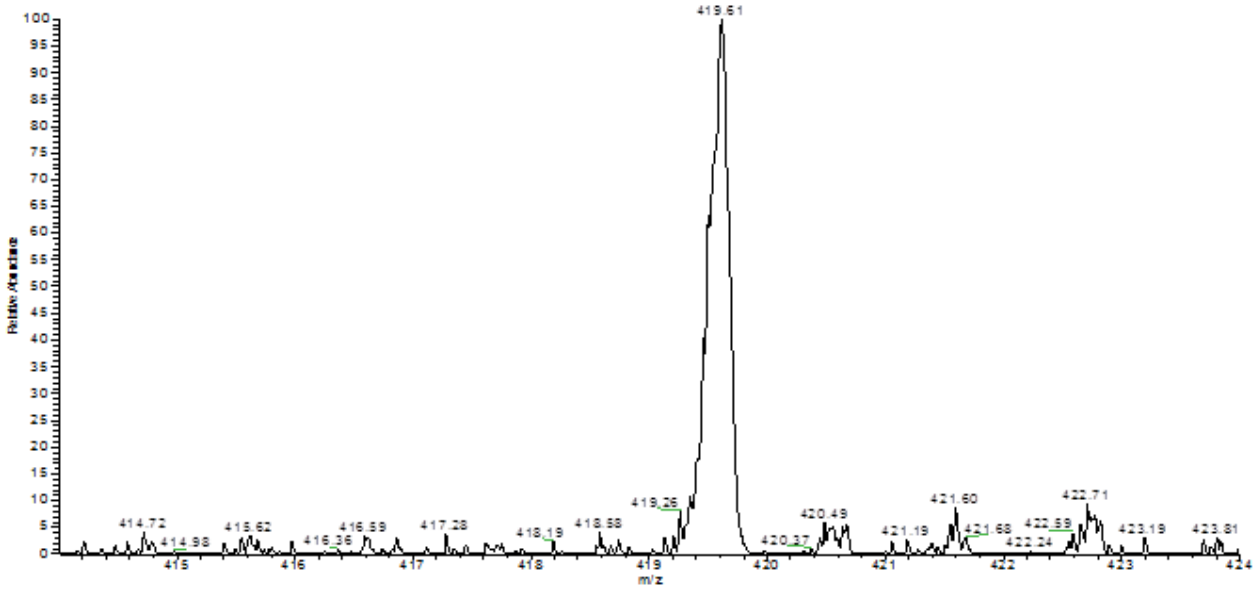

Fig. S26 Isotopic pattern of the dominant intermediate species of 419.61 m/z in the ESI-MS spectrum of complex **4** after adding two equivalent of Ce^{IV}.

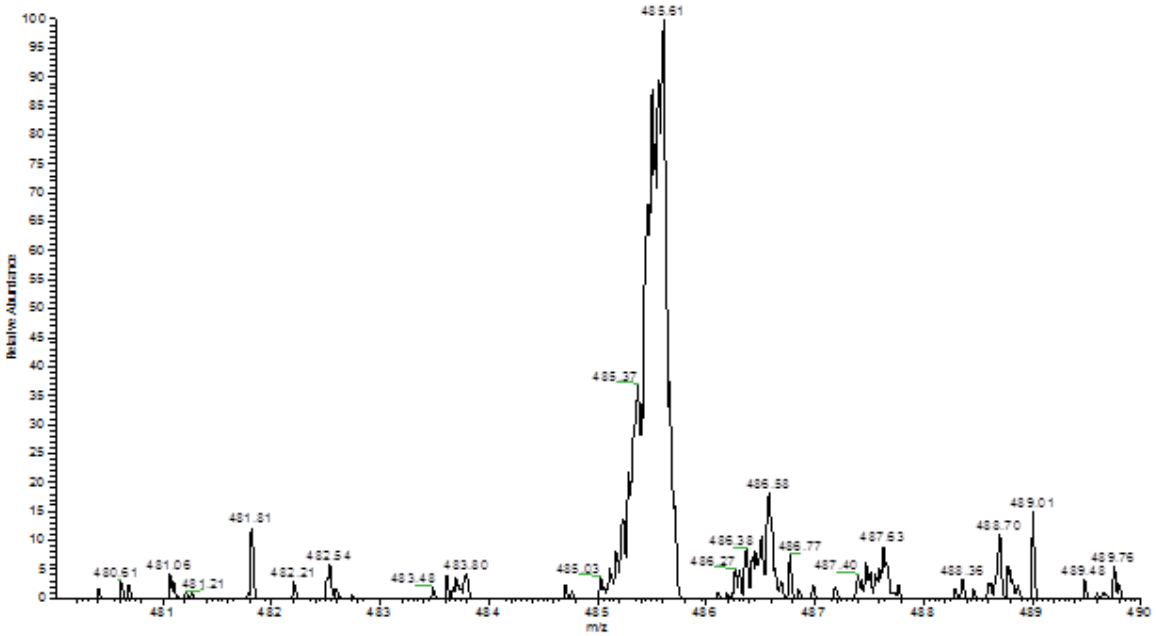

Fig. S27 Isotopic pattern of the dominant intermediate species of 485.61 m/z in the ESI-MS spectrum of complex **4** after adding two equivalent of Ce^{IV}.

6. UV-Vis studies of complex 1 to 4

6.1 UV-Vis as a function of pH

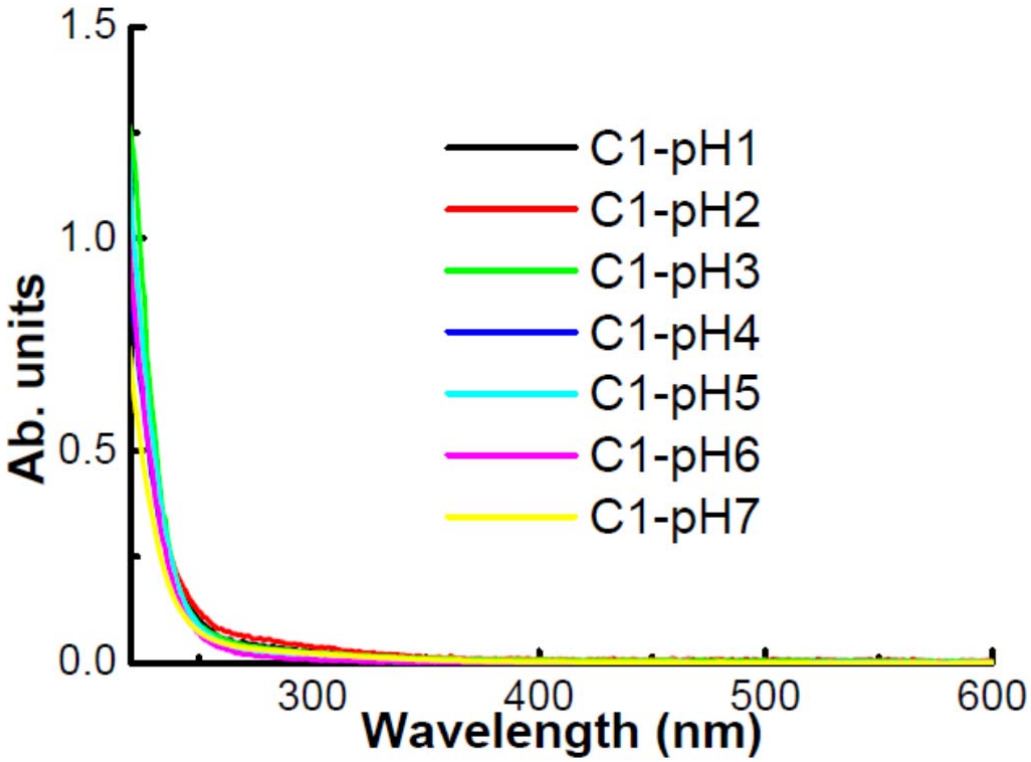

Fig. S28 UV-Vis spectrum of **1** as a function of pH.

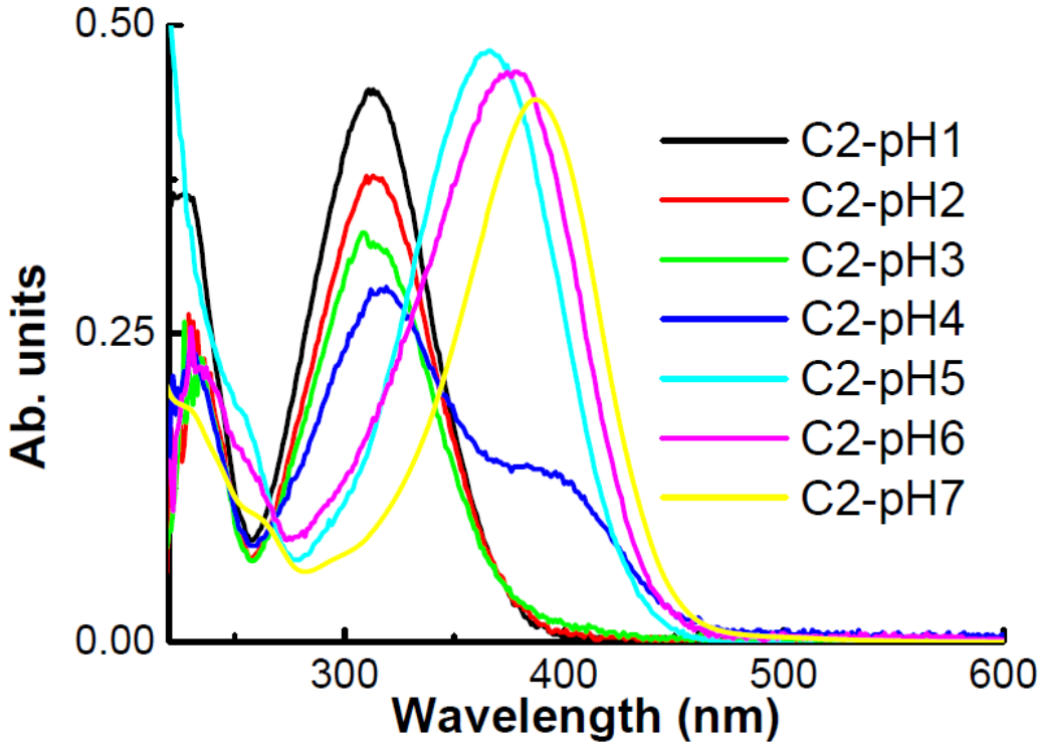

Fig. S29 UV-Vis spectrum of **2** as a function of pH.

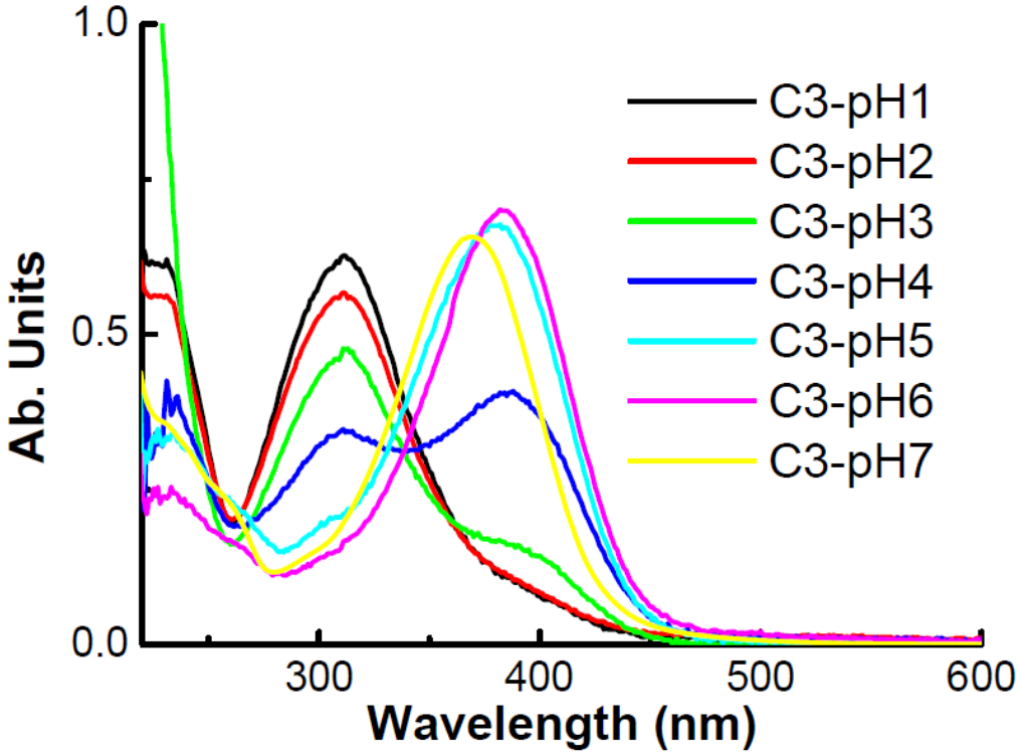

Fig. S30 UV-Vis spectrum of **3** as a function of pH.

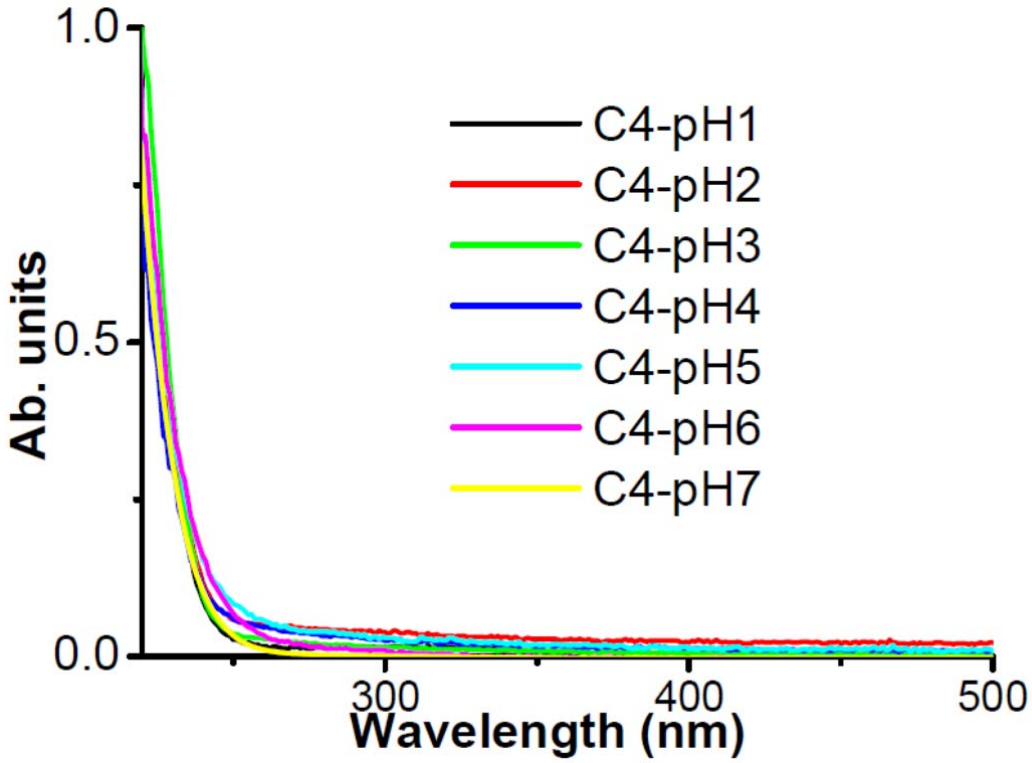

Fig. S31 UV-Vis spectrum of **4** as a function of pH.

6.2 UV-Vis after adding complexes 1 to 4 with CAN.

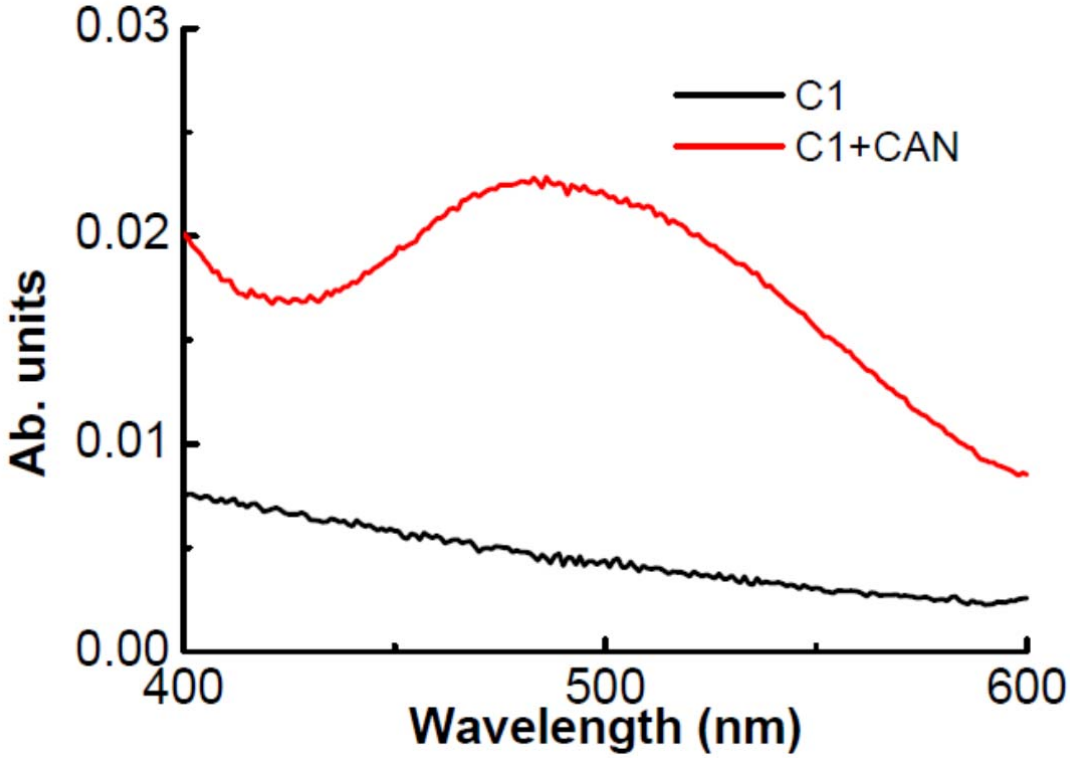

Fig. S32 Kinetically resolved absorption spectrum during reaction of one equivalent of complex **1** (0.02mM) with one equivalent of Ce^{IV} (0.02 mM) in H_2O.

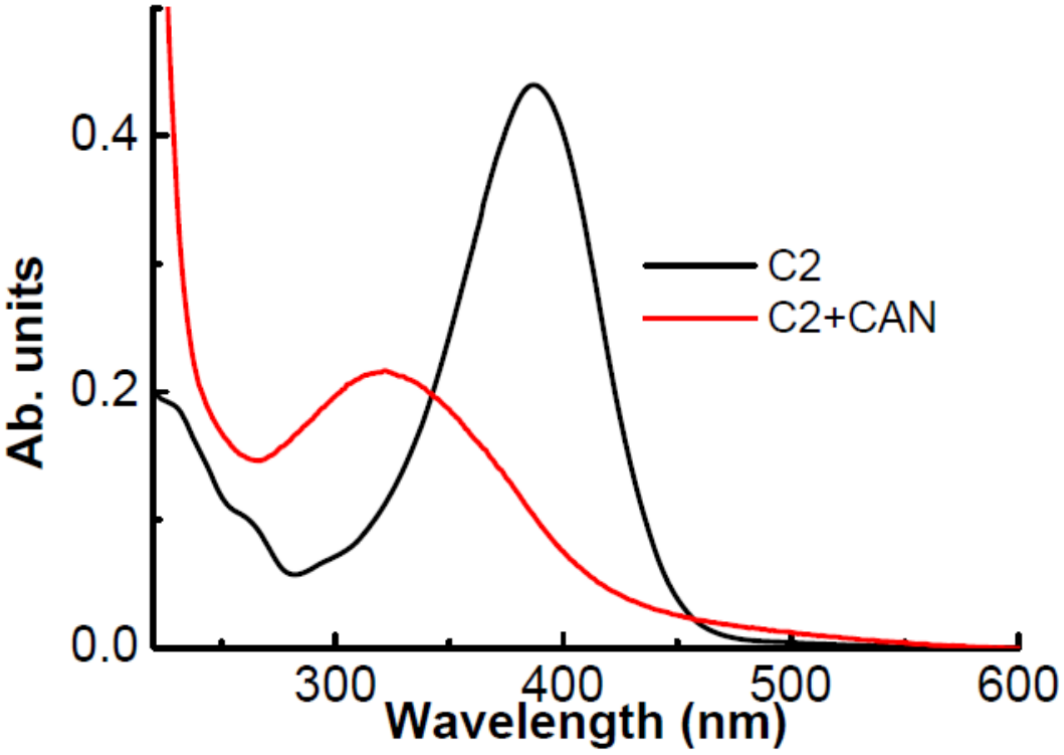

Fig. S33 Kinetically resolved absorption spectrum during reaction of one equivalent of complex **2** (0.02mM) with one equivalent of Ce^{IV} (0.02 mM) in H_2O.

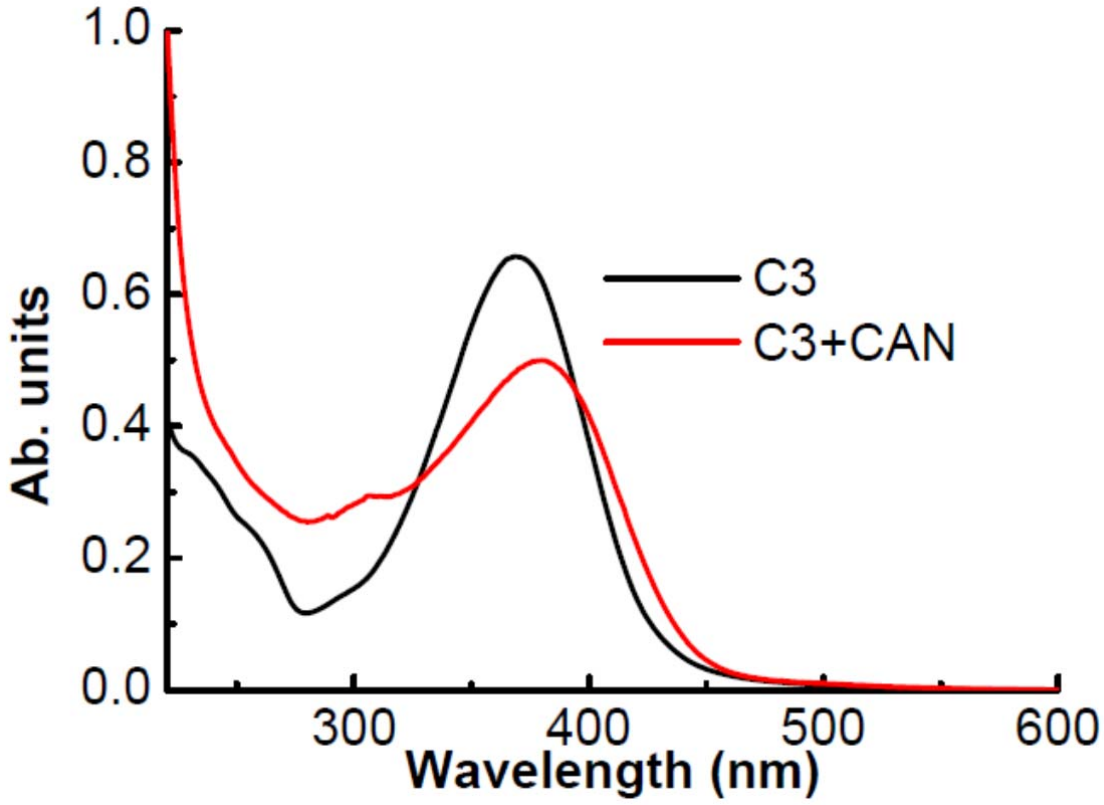

Fig. S34 Kinetically resolved absorption spectrum during reaction of one equivalent of complex **3** (0.02mM) with one equivalent of Ce^{IV} (0.02 mM) in H_2O.

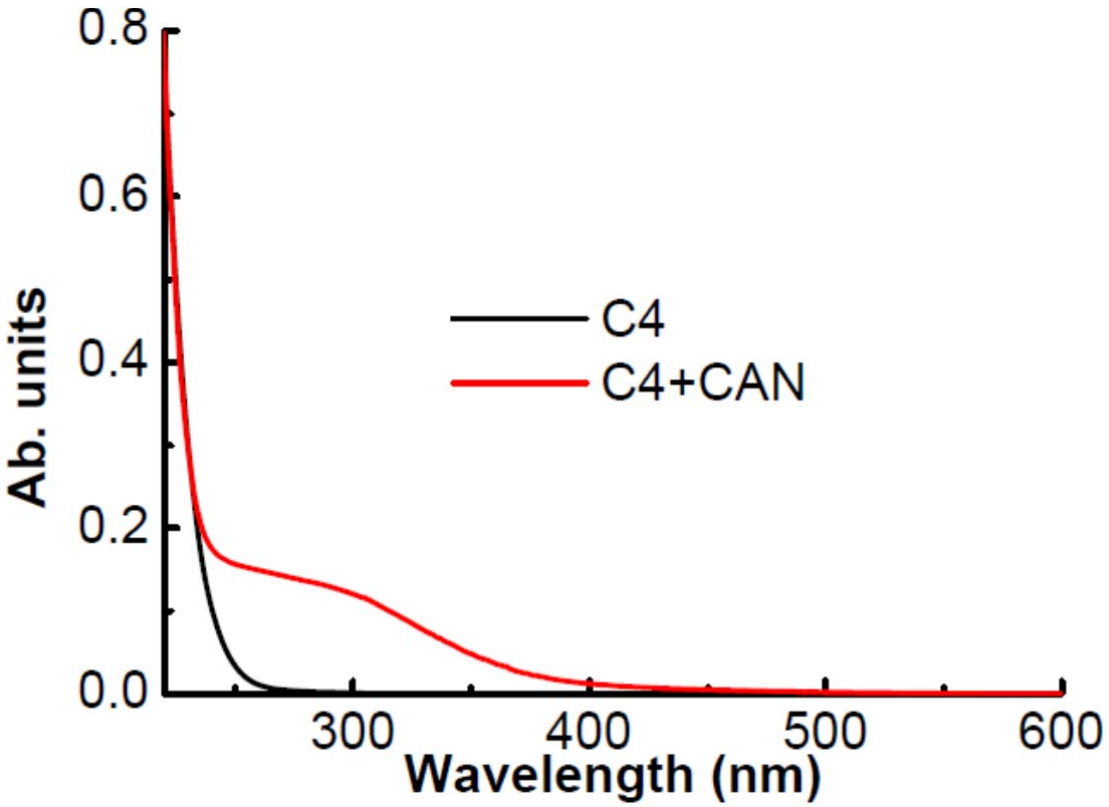

Fig. S35 Kinetically resolved absorption spectrum during reaction of one equivalent of complex **4** (0.02mM) with one equivalent of Ce^{IV} (0.02 mM) in H_2O.